Available online at www.sciencedirect.com
ScienceDirect
Applied Clay Science 35 (2007) 146–154
Applied CLAY Science
www.elsevier.com/locate/clay

Intercalation behavior of L-ascorbic acid into layered double hydroxides

Sumio Aisawa [a,*], Norihito Higashiyama [a], Satoshi Takahashi [a], Hidetoshi Hirahara [a], Daisaku Ikematsu [b], Hajime Kondo [b], Hirokazu Nakayama [c], Eiichi Narita [a]

[a] *Department of Frontier Materials and Function Engineering, Graduate School of Engineering, Iwate University, 4-3-5 Ueda, Morioka 020-8551, Japan*
[b] *Tayca Corporation, Osaka Research Laboratory, 1-3-47 Funamachi, Taisho-ku, Osaka 551-0022, Japan*
[c] *Department of Functional Molecular Chemistry, Kobe Pharmaceutical University, 4-19-1 Motoyama-kitamachi, Higashinada-ku, Kobe 658-8558, Japan*

Received 6 October 2005; received in revised form 2 September 2006; accepted 9 September 2006
Available online 17 October 2006

Abstract

The intercalation of L-ascorbic acid (ASA) into three kinds of layered double hydroxides, such as Mg–Al, Mg–Fe and Zn–Al LDHs, has quantitatively been investigated by the calcination-rehydration (reconstruction) and coprecipitation methods. The amount of ASA intercalated was considerably different by the LDH systems that was estimated to be ca. 0.40 mol/mol-M^{3+} for the Mg–Al and Mg–Fe systems by the reconstruction method. The Zn–Al system was hardly restored to the LDH structure by the rehydration reaction with the intercalation of ASA. ASA was also intercalated into the Mg–Al and Zn–Al LDHs by the coprecipitation method, while the intercalation of NO_3^- was observed in the Mg–Fe LDH. The basal spacing of the solid products were expanded to d_{003} = 0.84 (Mg–Al) and 0.86 (Mg–Fe) nm by the reconstruction method, 0.97 (Mg–Al) and 1.06 (Zn–Al) nm by the coprecipitation method, respectively, suggesting that ASA was intercalated into the LDHs. A large fraction of ASA was intercalated as reduced form after the light and heat resistance tests of the ASA/LDHs. This result confirmed that ASA was stabilized by the intercalation of the LDHs interlayer space. Furthermore, the intercalated ASA was easily deintercalated from the LDH interlayer space by the ion exchange method using CO_3^{2-}. It is expected that LDHs will be good host materials for safe storage of vitamins.

Keywords: Layered double hydroxides; L-ascorbic acid; Intercalation; Calcination-rehydration; Coprecipitation

1. Introduction

Clay minerals are focused on the synthesis of new organic–inorganic nanohybrid materials in recent years. A kind of clay minerals, layered double hydroxides (LDHs) are widely known as hydrotalcite-like compound and often called anionic clay comparing with the more conventional cationic clay. Hydrotalcite, $Mg_6Al_2(OH)_{16}CO_3{\cdot}4H_2O$, is the most frequently investigated anionic clay and is rarely found in nature. The chemical composition of LDHs is represented by general formula $[M^{2+}{}_{1-x}M^{3+}{}_x(OH)_2][A^{n-}{}_{x/n}{\cdot}yH_2O]$, where M^{2+} is a divalent cation such as Mg^{2+}, Zn^{2+}, Co^{2+}, Mn^{2+} and Cu^{2+}, M^{3+} is a trivalent cation such as Al^{3+}, Cr^{3+}, Co^{3+} and Fe^{3+}. A^{n-} is an ion exchangeable anion such as OH^-, Cl^-, NO_3^-, CO_3^{2-}, SO_4^{2-} and various organic anions. The x value is equal to the ratio $M^{3+}/(M^{2+}M^{3+})$,

* Corresponding author. Tel./fax: +81 19 621 6333.
E-mail address: aisawa@iwate-u.ac.jp (S. Aisawa).

0169-1317/$ - see front matter © 2006 Elsevier B.V. All rights reserved.
doi:10.1016/j.clay.2006.09.003

generally ranging between 0.20 and 0.33. This value is attributed to the charge density of the hydroxide basal layer, namely, anion exchange capacity (AEC). LDHs basal layer possesses a positive charge due to the trivalent cation substituted for the divalent cation, and the interlayer space is neutralized by the intercalation of anions with water molecules. The intercalation of various anions into LDHs has been attained by the following methods: coprecipitation, ion exchange, calcination-rehydration (reconstruction), thermal reaction and hydrothermal reactions (Miyata, 1980; Rives, 2001). Recently, LDHs are employed as the host material to synthesize a new organic–inorganic nanohybrid material and have received considerable attentions. The organic/LDHs nanohybrid materials have been investigated because the resulting intercalation compounds are expected to possess a novel nanostructure and new function (Ambrogi et al., 2001; de Melo et al., 2002; Choy et al., 2004; Kwak et al., 2004; del Arco et al., 2004a,b; Khan and O'Hare, 2002). A synthesis of biomolecule/LDH nanohybrid materials in particular has become of great interests. For a fact, the intercalation of the biomolecule such as nucleotide (Lotsch et al., 2001; Aisawa et al., 2005), deoxyribonucleic acid (Choy et al., 1999), amino acid (Whilton et al., 1997; Fudala et al., 1999; Aisawa et al., 2001, 2004) and polypeptide (Nakayama et al., 2004) into LDHs was described in order to prepare the biomolecule/LDH nanohybrid materials. Hydrotalcite is known to be biocompatible materials and has found pharmaceutical applications as antacid. In addition, anionic drug molecules have been intercalated into various LDHs, with an aim to determine the study of using these intercalation compounds as materials for storage, transport and ultimately controlled release of drug (He et al., 2004; del Arco et al., 2004a,b; Dupin et al., 2004; Li et al., 2004).

L-ascorbic acid (ASA) is known as vitamin C and helps some of our most important body systems. ASA assists the immune system to fight off foreign invaders and tumor cells and also supports the cardiovascular system by facilitating fat metabolism and protecting tissues from free radical damage. The solution of ASA is unsettled for natural light, thermal and alkaline conditions. Choy et al. reported the intercalation of vitamins such as vitamin A, C and E by the ion exchange and coprecipitation methods, moreover, the controlled release of their vitamins from vitamin/LDH was examined by ion exchange method (Hwang et al., 2001; Choy and Son, 2004). However, the durability, such as light and heat, of the intercalated ASA was not mentioned.

In the present study, the intercalation behavior of ASA into three kinds of LDHs, Mg−Al, Mg−Fe and Zn−Al systems, by the reconstruction and coprecipitation methods was investigated with the aim of synthesizing the ASA/LDHs. The quantitative determination of the intercalated ASA form, reduced and oxidized, after the light and heat resistance tests of the ASA/LDHs was studied with the intention of storing stability for ASA. In addition, the deintercalation of ASA from the ASA/LDHs, namely, release behavior of ASA, was also examined by the ion exchange method with CO_3^{2-}.

2. Experimental

2.1. Materials

ASA, other inorganic and organic reagents were purchased from Wako Pure Chemical Industries, Ltd., Japan and used without purification.

2.2. Intercalation of ASA by reconstruction method

The pristine CO_3/LDHs were synthesized by a standard coprecipitation method (Miyata, 1980). A mixed solution of 1 M $M^{2+}Cl_2$ and $M^{3+}Cl_3$ (M^{2+}/M^{3+}molar ratio=3/1, M^{2+}–M^{3+}=Mg−Al, Mg−Fe and Zn−Al) was instilled to 1 M Na_2CO_3 solution at 317 K with stirring and the suspension was aged at 317 K for 1 h. The solution pH was adjusted at 10 for the Mg−Al and Mg−Fe systems and 7.0 for the Zn−Al system by dropwise addition of 1 M NaOH solution during the instillation of the mixed solution. The precipitate was separated, washed with distilled water several times and added to 1 M Na_2CO_3 solution again. The slurry was aged again for 5 h with boiling. The resulting precipitate was collected by centrifugation, washed with distilled water three times and dried at 313 K for 24 h in a decompression oven. The chemical compositions of the CO_3/LDHs were shown in Table 1. The oxide precursors were prepared by the thermal decomposition of the CO_3/LDHs at 773 K for 2 h in a muffle furnace. Oxide precursor of 0.2 g was added to ASA solution (50 cm^3) with a desired concentration in a 100 cm^3 Erlenmeyer flask and shaken in a water bath at 298 K on proper times under a nitrogen atmosphere to prevent the formation of the CO_3/LDHs. The solid product was separated by filtration and washed with distilled water to remove excess adsorbed ASA. The solid product was dried at 313 K for 24 h in a decompression oven. The supernatant solution was subjected for the measurement of ASA concentration using a Shimadzu total organic carbon analyzer TOC-5000 (TOC).

2.3. Intercalation of ASA by coprecipitation method

A mixed solution of 0.1 M $M^{2+}(NO_3)_2$ and $M^{3+}(NO_3)_3$(M^{2+}/M^{3+}/ASA molar ratio=3/1/2) was instilled to 0.05 M ASA solution at 313 K with stirring under a nitrogen atmosphere to circumvent a contamination by atmospheric CO_2. The pH of ASA solution was regulated at 9.0 for the Mg−Al and Mg−Fe system and 7.0 for the Zn−Al system by dropwise addition of 0.1 M NaOH solution. The resulting precipitate was collected by centrifugation after aging for 1 h and washed three times with

Table 1
Chemical compositions of LDHs and reduced/oxidized ratio of ASA in ASA/LDHs

M^{2+}–M^{3} system	M^{2+}/M^{3+} molar ratio	ASA/M^{3+} molar ratio	Chemical composition	Reduced/oxidized ratio of ASA		
				Original	After light resistance	After heat resistance
CO_3/LDH						
Mg–Al	3.00	–	$[Mg_{0.75}Al_{0.25}(OH)_2][(CO_3)_{0.13}\bullet 0.72H_2O]$	–	–	–
Mg–Fe	3.00	–	$[Mg_{0.75}Fe_{0.25}(OH)_2][(CO_3)_{0.13}\bullet 0.84H_2O]$	–	–	–
Zn–Al	3.00	–	$[Zn_{0.75}Al_{0.25}(OH)_2][(CO_3)_{0.13}\bullet 0.88H_2O]$	–	–	–
Reconstruction						
Mg–Al	3.00	0.44	$[Mg_{0.75}Al_{0.25}(OH)_2][ASA_{0.11}(OH)_{0.14}\bullet 0.48H_2O]$	92/8	85/15	86/14
Mg–Fe	3.00	0.39	$[Mg_{0.75}Fe_{0.25}(OH)_2][ASA_{0.10}(OH)_{0.15}\bullet 0.57H_2O]$	86/14	76/24	75/25
Zn–Al	3.00	0.08	$[Zn_{0.75}Al_{0.25}(OH)_2][ASA_{0.02}(CO_3)_{0.04}(OH)_{0.15}\bullet yH_2O]$*	n. d.	–	–
Coprecipitation						
Mg–Al	3.00	0.48	$[Mg_{0.75}Al_{0.25}(OH)_2][ASA_{0.12}(NO_3)_{0.06}(OH)_{0.07}\bullet 0.66H_2O]$	94/6	84/16	86/14
Mg–Fe	3.00	0.12	$[Mg_{0.75}Fe_{0.25}(OH)_2][ASA_{0.03}(NO_3)_{0.20}(OH)_{0.02}\bullet 0.63H_2O]$	n. d.	–	–
Zn–Al	3.00	0.72	$[Zn_{0.75}Al_{0.25}(OH)_2][ASA_{0.18}(NO_3)_{0.03}(OH)_{0.04}\bullet 0.60H_2O]$	89/11	86/14	87/13
ASA	–	–	–	98/2	80/20	82/18

*The chemical composition of solid product was estimated as LDHs.

distilled water and dried at 313 K for 24 h in a decompression oven. The supernatant solution was evaluated for the measurement of ASA concentration by a TOC.

2.4. Light and heat resistance tests of ASA/LDHs

The light resistance test of the ASA/LDHs was carried out using a CO.FO.ME.GRA. SOLARBOX 1500e for 24 h at 303 K. SOLARBOX 1500e is xenon light exposure at 750 W/m^2 with 280 nm filter which simulates realistic natural sunlight. The heat resistance test of the ASA/LDHs, which sample was heated at 313 K for 30 days under an air atmosphere in an oven, was also examined.

2.5. Deintercalation of ASA from ASA/LDHs by ion exchange method

Deintercalation experiment was conducted of the ion exchange method using the ASA/Mg−Al and Zn−Al LDHs (coprecipitation method) and the ASA/Mg−Fe LDH (reconstruction method) for the ASA/LDHs. In the experiment for the deintercalation of ASA, 50 cm^3 of 0.05 M Na_2CO_3 solution was placed in a 100 cm^3 Erlenmeyer flask together with 0.1 g of the ASA/LDHs and shaken in a water bath set at 298 K for 24 h. The suspension was separated by centrifugation, washed three times with distilled water and dried in a decompression oven at 313 K for 24 h. The supernatant solution was determined the measurement of ASA concentration by a JASCO V-570 spectrophotometer (UV–Vis) at 265 nm, and the concentration of Na_2CO_3 was estimated by measuring TOC.

2.6. Characterization of solid products

Powder X-ray diffraction (XRD) measurements were performed on a Rigaku Rint 2200 powder X-ray diffractmeter, using a Cu Kα radiation at 20 mA, 40 kV and 2θ angle ranged from 2–60°. Fourier-transform infrared (FT-IR) spectra were obtained using a JASCO WS/IR 7300 FT-IR spectrophotometer by the KBr disk method. Solid-state ^{13}C cross-polarization and magic angle spinning nuclear magnetic resonance spectra (^{13}C CP/MAS NMR) spectra were obtained with Varian Unity INOVA-500 at 125.7 MHz. Chemical analysis data for the solid products were determined by a Shimadzu AA-6650 atomic absorption spectrometer (metal ion), a TOA Electronics IA-100 ion analyzer (NO_3^-), a TOC (ASA) and UV–Vis (ASA) after dissolution of the solid products in dilute HCl solution.

The quantitative determination of the intercalated ASA form, reduced and oxidized, was carried out using a hydrazine colorimetric determination method (Nihonyakugakkai, 1990). The solid product was added to metaphosphoric acid–acetic acid mixed solution. The sample solution was divided into three samples for test tubes as T1, T2 and T3, respectively. To oxidize ASA, 0.2 % 2,6-dichloroindophenol solution was added to T1 solution. Then metaphosphoric acid–thiourea mixed solution was added to T1–3, and 2,4-dinitrophenylhydrazine solution of 1 cm^3 was added to T1 and T2. 85% H_2SO_4 solution of 5 cm^3 was added to T1–3 after standing at 310 K for 3 h. Finally, 2,4-dinitrophenylhydrazine solution of 1 cm^3 was added to T3. The ratio of ASA form was determined by the sample solutions, T1 (total ASA), T2 (oxidized form) and T3 (blank), using a UV–Vis at 540 nm.

3. Results and discussion

3.1. Intercalation of ASA by reconstruction method

The time dependence on the amount of ASA intercalated by the M^{2+}–M^{3+}oxide precursors is shown in Fig. 1, in which the amount is expressed two units of

mmol/g-oxide (dotted line) and mol/mol-M^{3+}(line). The amount of ASA intercalated was continuously reached the equilibrium after about 120 h. The maximum amount was considerably different by the LDH systems, and that was estimated to be 2.41 mmol/g-oxide, 0.44 mol/mol-Al for the Mg–Al system, 1.92 mmol/g-oxide, 0.39 mol/mol-Fe for the Mg–Fe system and 0.32 mmol/g-oxide and 0.09 mol/mol-Al for the Zn–Al system, respectively. From the chemical compositions of the ASA/LDHs, a theoretical AEC of LDHs is 1.00 mol/mol-$M^{3+}$for monovalent anion. The initial solution pH was 7.0, and the equilibrium pH value rose to the region of 9.0–10.0 at 120 h. Acid-base equilibrium constants of ASA are pK_1=4.17 and pK_2=11.6 at 298 K in aqueous solution, indicating that ASA was intercalated as monovalent anion form into the LDHs. The chemical compositions of the solid product are shown in Table 1. In the Mg–Al and Mg–Fe systems, the amount of ASA intercalated, ca. 40%, was suitable for the AEC of both LDHs and the spare positive charge was neutralized by the intercalation of OH^-. However, ASA was hardly intercalated into the Zn–Al LDH, and CO_3^{2-} possessed 1/3 of AEC for the LDH. The broad and weak diffraction peak, 2θ=10–11°, was observed with the LDH structure as shown in Fig. 3i, meaning that the LDH structure is partly reconstructed by the intercalation of CO_3^{2-} and OH^-. In our previous report (Aisawa et al., 2003), D-ribose was not intercalated into the Zn–Al LDH by the reconstruction method because the rehydration reaction was hampered by the formation of a D-ribose/Zn complex on the surface of the Zn–Al oxide precursor. Besides, Kooli et al. (Kooli et al., 1997) reported that the Zn–Al oxide were not completely rehydrated because some Zn^{2+} could form an oxide phase or an amorphous zinc hydroxide phase undetectable by XRD. Therefore, ASA was hard to be intercalated into the Zn–Al LDH by the formation of ASA/Zn complex, zinc oxide and zinc hydroxide. We will make a report after conducting a further investigation on the intercalation of ASA into Zn–Al LDH by the reconstruction reaction.

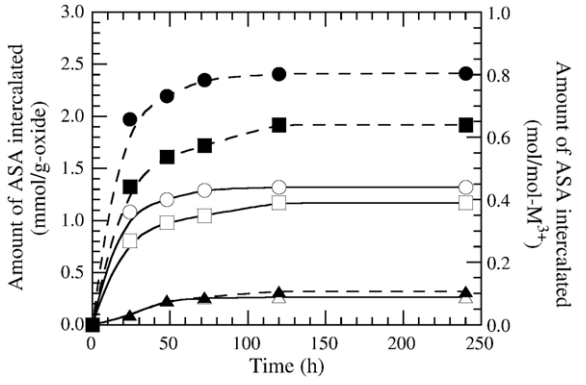

Fig. 1. Time dependence on amount of ASA intercalated by Mg–Al (●, ○), Mg–Fe (■, □) and Zn–Al oxide precursors (▲, △) at 298 K. Initial concentration of ASA: 50 mM, dotted-line: mmol/g-oxide, line: mol/mol-M^{3+}.

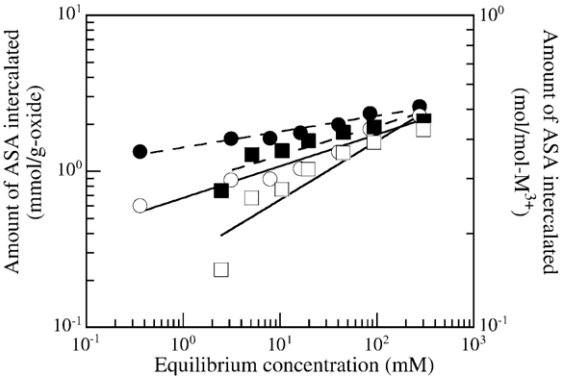

Fig. 2. Intercalation isotherms of ASA by Mg–Al (●, ○) and Mg–Fe (■, □) oxide precursors at 298 K after 120 h. Dotted-line: mmol/g-oxide, line: mol/mol-M^{3+}.

The amount (X/M) of ASA intercalated by the Mg–Al and Mg–Fe oxide precursors is examined at various initial concentrations and the results are shown in Fig. 2. The amount of ASA intercalated was found to rise slightly with an increase in ASA equilibrium concentration. In the both LDH systems, the Freundlich isotherm equation, log (X/M)=1/n (log C)+log k, is applicable. X (mmol and mol) is the amount of ASA intercalated, M (g-oxide and mol-M^{3+}) is the amount of the LDHs, C (mM) is the equilibrium concentration of ASA, k and n are the constants. The k and n values calculated from the intercept and slope of the isotherms in Fig. 2 and mean the adsorption strength and concentration dependence on adsorbent. The k and n values for the intercalation of ASA were k=1.42 mmol/g-oxide (0.26 mol/mol-Al) and n=9.85 for the Mg–Al system, k=0.82 mmol/g-oxide (0.17 mol/mol-Al) and n=5.32 for the Mg–Fe system. For most adsorbents n value is 2–3 (Moujahid et al., 2003), confirming that the Mg–Al and Mg–Fe LDHs are a good adsorbent of ASA. These k and n values mean that the Mg–Al and Mg–Fe LDHs have the ability to intercalate ASA in the wide ASA concentration region.

The XRD patterns of the pristine CO_3/LDHs, oxide precursors and solid products are shown in Fig. 3. The intensive main diffraction peaks of the CO_3/LDHs at d_{003}=0.76 and d_{006}=0.38 nm were observed in Fig. 3a, d and g, which values were in good agreement with that of hydrotalcite. By the calcination of these LDHs at 773 K for 2 h, the layered structure was demolished, which can be seen by the disappearance of some reflection peaks and the appearance of broad peak of periclase (MgO) and

zincite (ZnO) in Fig. 3b, e and h. The solid products were observed having the expanded LDH structure, $d_{003}=0.86$ and $d_{006}=0.43$ nm for the Mg–Al system and $d_{003}=0.84$ and $d_{006}=0.42$ nm for the Mg–Fe system, with the disappearance of periclase reflections, meaning that the Mg–Al and Mg–Fe oxide precursors were reconstructed the LDH structure by the rehydration reaction. As for the Zn–Al system, the broad and weak diffraction peak, $2\theta=10$–$11°$, was observed with the distinct diffraction peaks of zincite, indicating that the Zn–Al oxide precursor was hardly restored to the LDH structure by the rehydration reaction with intercalation of ASA. The schematic illustrations of the ASA/LDHs are shown in Fig. 4. Molecular size of ASA is calculated as 0.49 nm in length, 0.60 nm in wide and 0.36 nm in thickness. As the LDH basal layer is 0.48 nm in thickness, the interlayer

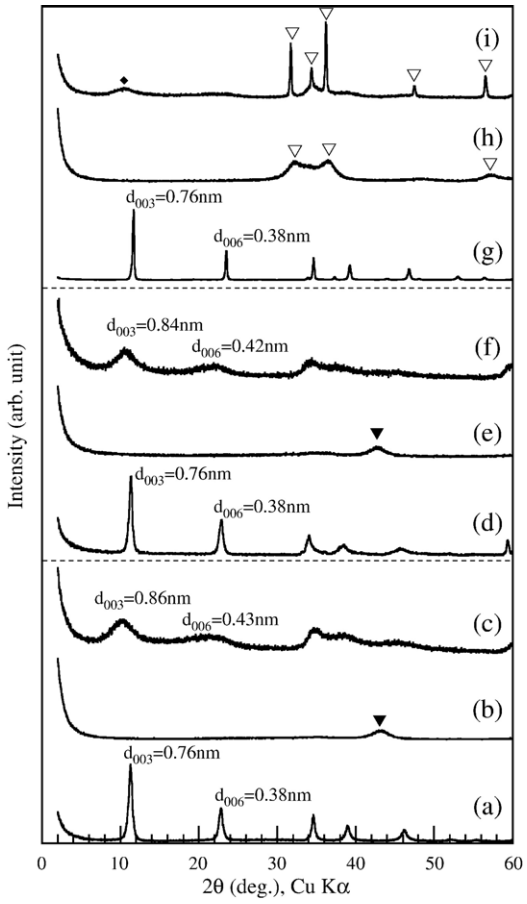

Fig. 3. XRD patterns of solid products (reconstruction). (a) CO_3/Mg–Al LDH, (b) Mg–Al oxide precursor, (c) ASA/Mg–Al LDH, (d) CO_3/Mg–Fe LDH, (e) Mg–Fe oxide precursor, (f) ASA/Mg–Fe LDH, (g) CO_3/Zn–Al LDH, (h) Zn–Al oxide precursor and (i) ASA/Zn–Al LDH. ASA concentration: 0.05 M, reaction time: 120 h. ▼: Periclase (MgO), ▽: zincite (ZnO), ♦: LDH structure.

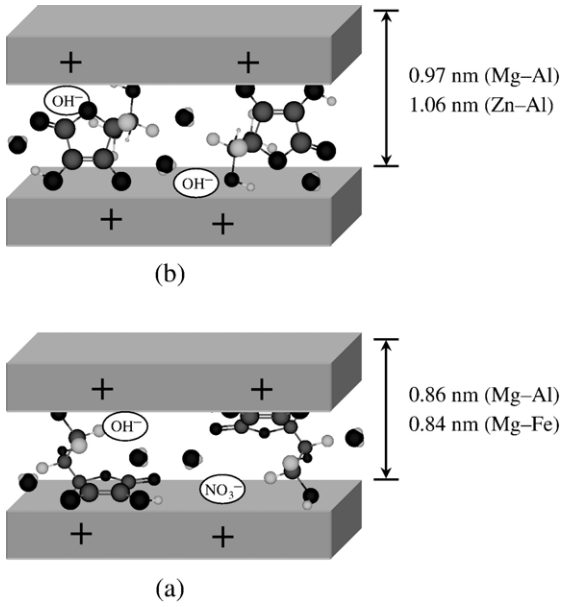

Fig. 4. Schematic illustrations of ASA/LDHs. (a) reconstruction method and (b) coprecipitation method.

distance of the ASA/LDHs was estimated to 0.38 nm for the Mg–Al LDH and 0.36 nm for the Mg–Fe LDH, suggesting that ASA was horizontally placed to the LDH basal layer as shown in Fig. 4a. However, the ASA/LDHs did not constitute a well-organized stacking arrangement, because OH^- was co-intercalated within the ASA/LDHs interlayer space.

The FT-IR spectra of the pristine CO_3/LDHs and the resulting ASA/LDHs are shown in Fig. 5. Broad absorption peaks in the 1635–1655 and 2800–3600 cm^{-1} regions are assigned to O–H group stretching and deformation vibration of the hydroxide basal layer and interlayer water molecules. The strong peak at 1375 cm^{-1} is attributed to C–O stretching mode of the intercalated CO_3^{2-} (Fig. 5a, c and e). The low frequency region is associated with M–O and O–M–O stretching modes in the LDH basal layer. The ASA/LDHs exhibits the FT-IR peaks characteristic of both ASA and LDH basal layer. The broad and weak peaks in the 1000–1165 and 1635–1655 cm^{-1} regions were characteristic of C═O and C–O–C stretching in ASA (Fig. 5b, d and f). The absorption peaks at 1389 and 1393 cm^{-1}, assigned to C–O in Fig. 5b and d, were shifted from 1320 cm^{-1} for naked ASA after the intercalation because the electrostatic force of attraction increased between the negative ASA and the positive LDH basal layer. The ASA/Zn–Al LDH showed the absorption peaks of C–O and O–H stretching due to the co-intercalated CO_3^{2-} and LDH sheets. The absorption peaks of the intercalated

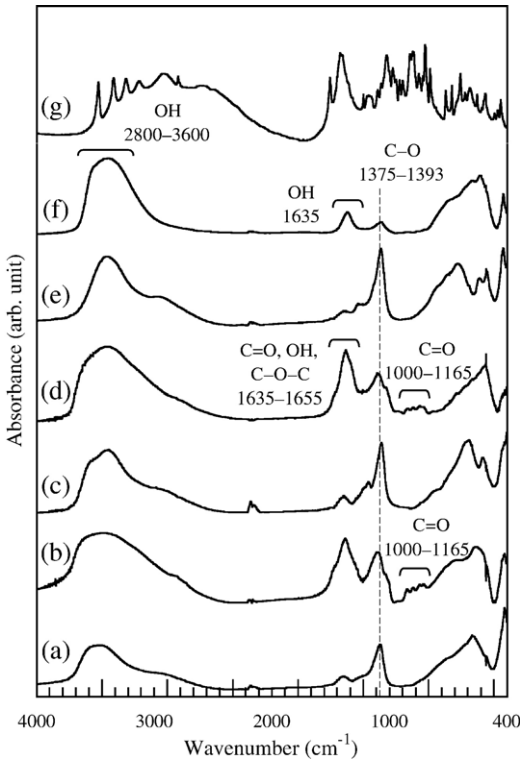

Fig. 5. FT-IR spectra of solid products (reconstruction). (a) CO_3/Mg–Al LDH, (b) ASA/Mg–Al LDH, (c) CO_3/Mg–Fe LDH, (d) ASA/Mg–Fe LDH, (e) CO_3/Zn–Al LDH, (f) ASA/Zn–Al LDH and (g) ASA. ASA concentration: 0.05 M, reaction time: 120 h.

ASA were hardly observed, because the amount of ASA intercalated was quite small as 0.12 mmol/g-oxide.

3.2. Intercalation of ASA by coprecipitation method

In this section, the intercalation of ASA into the LDH precipitates was investigated by the coprecipitation method. The chemical compositions of the ASA/LDHs are shown in Table 1. The amounts of ASA intercalated were 0.48 mol/mol-Al for the Mg–Al system, 0.12 mol/mol-Fe for the Mg–Fe system and 0.72 mol/mol-Al for the Zn–Al system. The molar ratios of the ASA/LDHs almost agreed with the stoichiometry of LDHs, when NO_3^- and OH^- were co-intercalated to supplement an excessive electric charge of the LDHs basal layer.

The XRD patterns of the ASA/LDHs are presented in Fig. 6. The broad diffraction peak at $d_{003}=0.97$ nm was observed with the LDH structure in the ASA/Mg–Al LDH. In the Mg–Fe system, the weak diffraction peaks, $d_{003}=0.86$ and $d_{006}=0.43$ nm, are observed with LDH structure in Fig. 6b. From the results of the chemical composition and d-values of the solid products, NO_3^- was intercalated into the LDH. A part of ASA was located on the surface of the NO_3/Mg–Fe LDH as shown in Table 1. The diffraction peaks with expanding LDH structure, $d_{003}=1.06$ and $d_{006}=0.52$ nm, are observed in the ASA/Zn–Al LDH as shown in Fig. 6c. These values are in good agreement with those of the ASA/Zn–Al LDH in previous report (Choy and Son, 2004). The ASA/Mg–Al and Zn–Al LDHs possess an expanding LDHs structure, indicating that ASA was intercalated into the LDH. As the thickness of the LDHs basal layer is 0.48 nm, the interlayer distance of the ASA/LDHs was estimated to 0.49 nm for the Mg–Al system and 0.58 nm for the Zn–Al system, supporting that ASA existed vertical to the LDH basal layer. A schematic illustration of the possible arrangement is shown in Fig. 4b. Then the basal spacing of the ASA/Zn–Al LDH was more expanded than that of the ASA/Mg–Al LDH. Acid-base equilibrium constants of ASA are $pK_1=4.17$ and $pK_2=11.6$, the coprecipitation pH of ASA was executed at pH 9.0 for the Mg−Al system and 7.0 for the Zn−Al system. The difference of the basal spacing of the ASA/LDHs is due to the electrostatic force of attraction between the negative intercalated ASA and the positive LDH basal layer. Taking into account ASA solution pH, negatively electrostatic force of ASA was increased with rising of solution pH, because ASA was easily deprotonated. Moreover, in the Zn–Al LDH, the amount of ASA intercalated was 0.24 (ASA/Al^{3+}molar ratio) greater than that of the Mg–Al LDH. The interlayer distances of the ASA/LDHs and the orientation of the intercalated ASA were also caused by the amount of ASA intercalated.

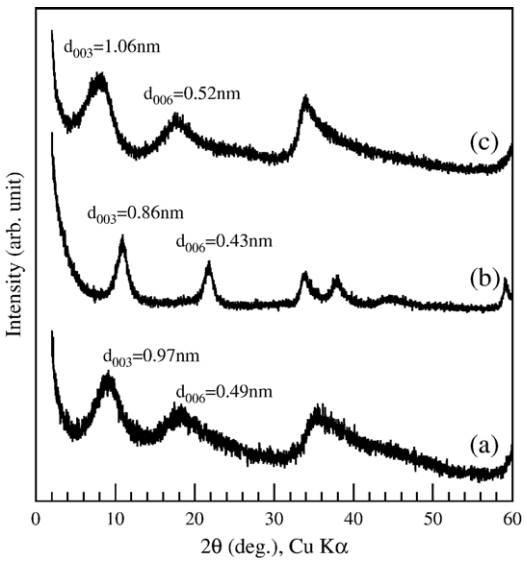

Fig. 6. XRD patterns of solid products (coprecipitation). (a) ASA/Mg–Al LDH, (b) ASA/Mg–Fe LDH and (c) ASA/Zn–Al LDH.

The FT-IR spectra of the ASA/LDHs are shown in Fig. 7. In each case, a broad absorption peak in the 2800–3600 cm^{-1} region is assigned to O–H group stretches of hydroxide basal layer and interlayer water. The weak absorption peaks of alkyl C–H stretch in the 2900–3000 cm^{-1} region, the strong absorption peaks of C═O stretch at 1640 cm^{-1}, the medium absorption peaks of C–O stretch at 1325 cm^{-1} and weak absorption peak of ν-OH at 1125 cm^{-1} were observed due to the intercalation of ASA into the Mg–Al and Zn–Al LDH. The co-intercalated NO_3^- gives an absorption peak at 1385 cm^{-1} in the ASA/LDHs, especially in the Mg–Fe LDH. The absorption peaks of the lattice vibration modes are attributed to M–O and O–M–O vibrations in the low-frequency region.

The ^{13}C CP/MAS NMR spectra of the ASA/Mg–Al and Zn–Al LDHs are shown in Fig. 8. As a reference, the chemical shift values of ASA in D_2O were observed at 174.0 (C-1), 118.7 (C-2), 156.2 (C-3), 77.0 (C-4), 69.8 (C-5) and 62.9 (C-6) ppm. The chemical shift values of the ASA/Mg–Al LDH were shown at 181.5 (C-1), 121.2 (C-2), 169.2 (C-3), 73.5 (C-4 and 5) and 65.3 (C-6) ppm. In the case of the ASA/Zn–Al LDH, the chemical shift values were generally corresponded to

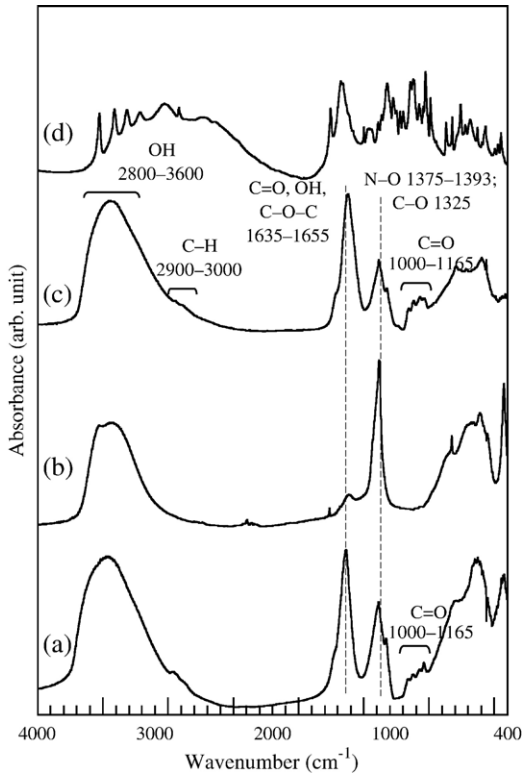

Fig. 7. FT-IR spectra of solid products (coprecipitation). (a) ASA/Mg–Al LDH, (b) ASA/Mg–Fe LDH, (c) ASA/Zn–Al LDH and (d) ASA.

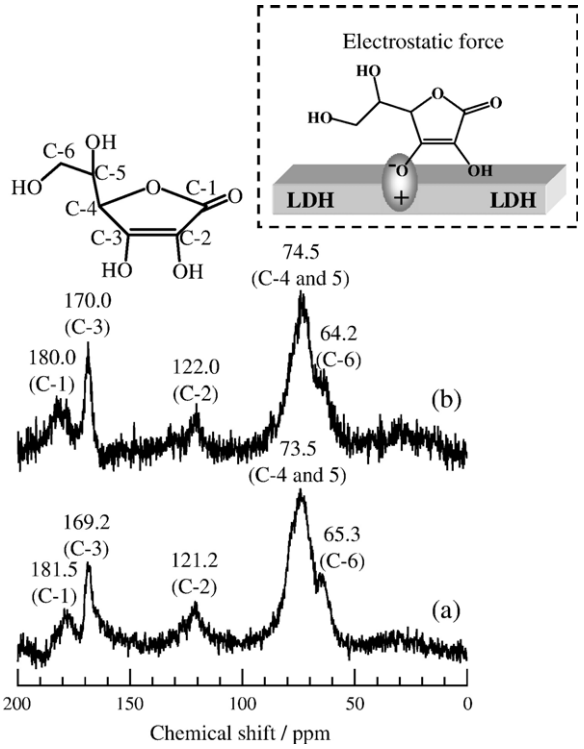

Fig. 8. ^{13}C CP/MAS NMR spectra of solid products (coprecipitation). (a) ASA/Mg–Al LDH and (b) ASA/Zn–Al LDH.

that of the ASA/Mg–Al LDH. The chemical shift values of the intercalated ASA were entirely shifted to upfield in comparison with naked ASA. The chemical shift value of ASA at 156.2 (C-5) ppm was greatly shifted to 169.2 ppm for the Mg–Al LDH and 170.0 ppm for the Zn–Al LDH, supporting that the electrostatic force of attraction was strongly acted between the intercalated negative ASA and the positive LDH basal layer.

3.3. Light and heat resistance tests of ASA/LDHs

ASA is well-known to be easily oxidized in air atmosphere with heat and light. Then the quantitative determination of the intercalated ASA form, reduced and oxidized, after the light and heat resistance tests of the ASA/LDHs was evaluated, and the results are shown in Table 1. As a reference, the naked ASA form was also examined, and it was found to keep as reduced form. As compare with the naked ASA, the intercalated ASA was slightly oxidized during the intercalation reaction at weak alkaline condition. In the reconstruction method, ASA reduced form content in the Mg–Al LDH was higher than that of in the Mg–Fe LDH, considering that a part of Fe^{3+} was eluted from the Mg–Fe oxide precursor and was reduced by ASA during the reconstruction

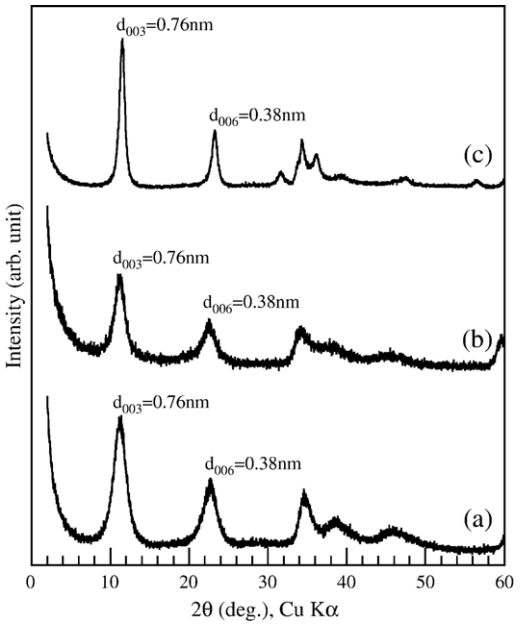

Fig. 9. XRD patterns of solid products after ASA deintercalated. (a) ASA/Mg–Al LDH, (b) ASA/Mg–Fe LDH and (c) ASA/Zn–Al LDH.

reaction. In the case of the coprecipitation method, ASA reduced/oxidized ratios of the ASA/LDHs were 94/6 for the Mg–Al LDH and 89/11 for the Zn–Al LDH. The naked ASA was oxidized by the light and heat resistance tests, when ASA reduced form decreased by 80 and 82 from 98, respectively. The intercalated ASA was also oxidized after the light and heat resistance tests, however the oxidation rates of the intercalated ASA were slower than that of the naked ASA and influenced by the kind of LDH systems. He et al. (2004), Guo et al. (2006) and Tronto et al. (2006) reported that the light resistance and thermal stability of organic guests were improved by intercalation in the layered host. On the other hand, the basicities of the Mg–M^{3+} LDHs advanced the oxidation of the intercalated ASA, consequently the Zn–Al LDH possesses a good host material for storage of ASA. These results confirmed that the oxidation of ASA was inhibited by the intercalation into the LDHs interlayer space.

3.4. Deintercalation of ASA from ASA/LDHs

The deintercalation of ASA from the ASA/LDHs by the ion exchange with CO_3^{2-} was investigated in order to release the intercalated ASA. The degree of ASA deintercalation was estimated as 92% for the Mg–Al system, 88% for the Mg–Fe system and 82% for the Zn–Al system after 24 h. These results confirmed that a large fraction of the intercalated ASA was deintercalated from the ASA/LDHs by the simple and easy ion exchange method. The XRD patters of the solid product are shown in Fig. 9. The diffraction peaks of the solid products were observed at $d_{003}=0.76$ and $d_{006}=0.38$ nm which agreed with those of the CO_3/LDHs. The decrease in the d-value supported that ASA was deintercalated from the ASA/LDHs. According to the FT-IR spectra of the solid products (data not shown), the absorption peaks of the intercalated ASA at 2900–3000, 1640, 1325 and 1125 cm^{-1} completely disappeared after the deintercalation. Moreover, the quantitative determination of the deintercalated ASA form was carried out, a large fraction of the released ASA was found to keep the reduced form.

4. Conclusion

We concluded some of the important and interesting findings of the intercalation behavior of ASA into the Mg–Al, Mg–Fe and Zn–Al LDHs by the reconstruction and coprecipitation methods and the light and heat resistance tests of the ASA/LDHs as follows. (I) The ASA/LDHs can be prepared by the both methods except the Mg–Fe LDH on the coprecipitation method and the Zn–Al LDH on the reconstruction method. (II) The ASA/LDHs showed the expanded LDH structures with (003) spacing of 0.84–1.06 nm. From the interlayer distances of the ASA/LDHs, ASA existed horizontal or vertical orientation in the LDHs interlayer space. (III) The intercalated ASA was mostly contained as reduced form after the light and heat resistance tests, indicating that ASA was stabilized by the intercalation into the LDHs interlayer space. (IV) ASA was easily deintercalated from the ASA/LDHs by the ion exchange method using Na_2CO_3 solution, and the deintercalated ASA was found to keep the reduced form. (V) LDHs have protection abilities from light and heat and may function as a molecular container.

Acknowledgement

This work was supported by a Grant-in-Aid for Scientific Research from the Ministry of Education, Culture, Sports, Science and Technology, Japan (No. 16550164).

References

Aisawa, S., Takahashi, S., Ogasawara, W., Umetsu, Y., Narita, E., 2001. Direct intercalation of amino acids into the layered double hydroxides by coprecipitation. J. Solid State Chem. 162, 52–62.

Aisawa, S., Hirahara, H., Ishiyama, K., Ogasawara, W., Umetsu, Y., Narita, E., 2003. Sugar-anionic clay composite materials: intercalation of pentoses in layered double hydroxide. J. Solid State Chem. 174, 342–348.

Aisawa, S., Kudo, H., Hoshi, T., Takahashi, S., Hirahara, H., Umetsu, Y., Narita, E., 2004. Intercalation behavior of amino acids into Zn–Al layered double hydroxide by calcination-rehydration reaction. J. Solid State Chem. 177, 3987–3994.

Aisawa, S., Ohnuma, Y., Hirose, K., Takahashi, S., Hirahara, H., Narita, E., 2005. Intercalation of nucleotide for layered double hydroxides by ion-exchange reaction. Appl. Clay Sci. 28, 137–145.

Ambrogi, V., Fardella, G., Grandolini, G., Perioli, L., 2001. Intercalation compounds of hydrotalcite-like anionic clays with antiinflammatory agents—I. Intercalation and in vitro release of ibuprofen. Int. J. Pharm. 220, 23–32.

Choy, J.-H., Son, Y.-H., 2004. Intercalation of vitamer into LDH and their controlled release properties. Bull. Korean Chem. Soc. 25, 122–126.

Choy, J.-H., Kwak, S.-Y., Park, J.-S., Jeong, Y.-J., Portier, J., 1999. Intercalative nanohybrids of nucleoside monophosphates and DNA in layered metal hydroxide. J. Am. Chem. Soc. 121, 1399–1400.

Choy, J.-H., Jung, J.-S., Oh, J.-M., Park, M., Jeong, J., Kang, Y.-K., Han, O.-J., 2004. Layered double hydroxide as an efficient drug reservoir for folate derivatives. Biomaterials 25, 3059–3064.

del Arco, M., Cebadera, E., Gutiérrez, S., Martín, C., Montero, M.J., Rocha, J., Sevilla, M.A., 2004a. Mg, Al layered double hydroxides with intercalated indomethacin: synthesis, characterization, and pharmacological study. J. Pharm. Sci. 93, 1649–1657.

del Arco, M., Gutiérezze, S., Martín, C., Rives, V., Rocha, J., 2004b. Synthesis and characterization of layered double hydroxides (LDH) intercalated with non-steroidal anti-inflammatory drugs (NSAID). J. Solid State Chem. 177, 3954–3962.

de Melo, J.V., Cosnier, S., Mousty, C., Martelet, C., Jaffrezic-Renault, N., 2002. Urea biosensors based on immobilization of urease into two oppositely charged clays (laponite and Zn–Al layered double hydroxides). Anal. Chem. 74, 4037–4043.

Dupin, J.-C., Martinez, H., Guimon, C., Dumitriu, E., Fechete, I., 2004. Intercalation compounds of Mg–Al layered double hydroxides with dichlophenac: different methods of preparation and physico-chemical characterization. Appl. Clay Sci. 27, 95–106.

Fudala, Á., Pálinkó, I., Kiricsi, I., 1999. Preparation and characterization of hybrid organic–inorganic composite materials using the amphoteric property of amino acids: amino acid intercalated layered double hydroxide and montmorillonite. Inorg. Chem. 38, 4653–4658.

Gou, S., Evans, D.G., Li, D., 2006. Preparation of C.I. Pigment 52:1 anion-pillared layered double hydroxide and the thermo- and photostability of the resulting intercalated material. J. Phys. Chem. Solids 67, 1002–1006.

He, Q., Yin, S., Sato, T., 2004. Synthesis and photochemical properties of zinc–aluminum layered double hydroxide/organic UV ray absorbing molecule/silica nanocomposites. J. Phys. Chem. Solids 65, 395–402.

Hwang, S.-H., Han, Y.-S., Choy, J.-H., 2001. Intercalation of functional organic molecules with pharmaceutical, cosmeceutical and nutraceutical functions into layered double hydroxides and zinc basic salts. Bull. Korean Chem. Soc. 22, 1019–1022.

Khan, A.I., O'Hare, D., 2002. Intercalation chemistry of layered double hydroxides: recent developments and applications. J. Mater. Chem. 12, 3191–3198.

Kooli, F., Depège, C., Ennaqadi, A., de Roy, A., Besse, J.P., 1997. Rehydration of Zn–Al layered double hydroxides. Clay Clay Miner. 45, 92–98.

Kwak, S.-Y., Kriven, W.M., Matthew, M.A., Wallig, A., Choy, J.-H., 2004. Inorganic delivery vector for intravenous injection. Biomaterials 25, 5995–6001.

Li, B., He, J., Evans, D.G., Duan, X., 2004. Enteric-coated layered double hydroxides as a controlled release drug delivery system. Int. J. Pharm. 287, 89–95.

Lotsch, B., Millange, F., Walton, R.I., O'Hare, D., 2001. Separation of nucleoside monophosphates using preferential anion exchange intercalation in layered double hydroxides. Solid State Sci. 3, 883–886.

Miyata, S., 1980. Physico chemical properties of synthetic hydrotalcites in relation to composition. Clays Clay Miner. 28, 50–56.

Moujahid, E.M., Inacio, J., Besse, J.P., Leroux, F., 2003. Adsorption of styrene sulfonate vs. polystyrene sulfonate on layered double hydroxides. Microporous Mesoporous Mater. 57, 37–46.

Nakayama, H., Wada, N., Tsuhako, M., 2004. Intercalation of amino acids and peptides into Mg–Al layered double hydroxide by reconstruction method. Int. J. Pharm. 269, 469–478.

Nihonyakugakkai (Ed.), 1990. Eiseishikenhou-chuukai. Kanehara, Tokyo.

Rives, V. (Ed.), 2001. Layered Double Hydroxides: Present and Future. Nova Science Publishers, New York.

Tronto, J., Leroux, F., Dubois, M., Taviot-Gueho, C., Naal, Z., Klein, S.I., Valim, J.B., 2006. New layered double hydroxides intercalated with substituted pyrroles. 2,3-(Pyrrol-1-yl)-propanoate and 7-(pyrrol-1-yl)-heptanoate LDHs. J. Phys. Chem. Solids 67, 973–977.

Whilton, N.T., Vickers, P.J., Mann, S., 1997. Bioinorganic clays: synthesis and characterization of amino- and polyamino acid intercalated layered double hydroxides. J. Mater. Chem. 7, 1623–1629.